PROBABILISTIC LIFE-CYCLE COST ANALYSIS FOR THE CONSTRUCTION AND MAINTENANCE OF REINFORCED CONCRETE STRUCTURES

Hideyuki KOBAYASHI*
East Japan Railway Company*

***ABSTRACT*:** This study develops a probabilistic framework that can estimate the Life-Cycle Cost (LCC) of reinforced concrete (RC) structures under various construction and maintenance scenarios. This paper first describes a chloride-induced deterioration model to predict the service-life of RC structures. Then, the Monte-Carlo Simulation method is applied to the deterioration model and subsequent LCC estimation to assess the uncertainties of input variables probabilistically.

This paper also discusses a case study in which the probabilistic Life-Cycle Cost Analysis (LCCA) framework is applied to a RC viaduct. The case study compares the potential ranges of LCC among eight different life-cycle scenarios. This study suggests that the developed probabilistic LCCA framework can be used as an effective decision-making method to identify the most cost-effective life-cycle scenario of RC structures, while reflecting the risk-attitude of the decision-maker.

KEYWORDS: Life-Cycle Cost Analysis, Reinforced Concrete, Monte-Carlo Simulation

1. INTRODUCTION

In recent decades, the deterioration of concrete infrastructures has become a serious social issue in many countries. In response, a variety of durable construction materials and innovative maintenance methods have been developed to enhance or to sustain the durability of concrete structures, diversifying the life-cycle design of structures. Accordingly, Life-Cycle Cost Analysis (LCCA) has been recognized as an effective method for selecting the cost-effective life-cycle scenario of structures from a long-term perspective.

However, despite the uncertain nature of the concrete deterioration processes and future expenditures, the traditional deterministic LCCA cannot evaluate these uncertainties in estimating the service-life and LCC of structures. Instead, a decision-maker produces a series of *best guesses* of the values for each variable and computes a single deterministic result. These approaches are straightforward and simple, but the selection of life-cycle scenario is made based only on a single output without an appropriate assessment of the potential risks of LCC increase.

Given this context, this study aims to develop a probabilistic LCCA framework for reinforced concrete (RC) structures under various construction and maintenance scenarios. This paper first describes a chloride-induced concrete deterioration model based on previous studies. Then, the Monte-Carlo Simulation method is applied to the deterioration model and subsequent LCC estimation to assess the uncertainties of input variables probabilistically. This study also conducts a case study in which the developed LCCA framework is applied to a RC viaduct under eight different life-cycle scenarios.

2. DETERIORATION MODEL

2.1 General Scheme

Figure 1 illustrates the deterioration process of RC structures (Japan Society of Civil Engineers (JSCE) 2001). The overall process is composed of four stages: initiation, propagation, acceleration, and deterioration, depending on the degree of reinforcement corrosion and crack development in the covering concrete.

This study focuses only on the chloride-induced concrete deterioration, which is one of the most dominant deterioration causes for RC structures, and develops a deterioration model based on this JSCE's concept. With this model, we can estimate following three time periods to identify the points in time when a structure transits to the next deterioration stage.

1) The elapsed time prior to the initiation of reinforcement corrosion (*time-to-corrosion,* t_c)
2) The elapsed time before cracks are induced into the covering concrete (*time-to-cracking,* t_{cr})
3) The elapsed time before the cracks expand to the threshold width (*time-to-crack-expansion,* t_{ce})

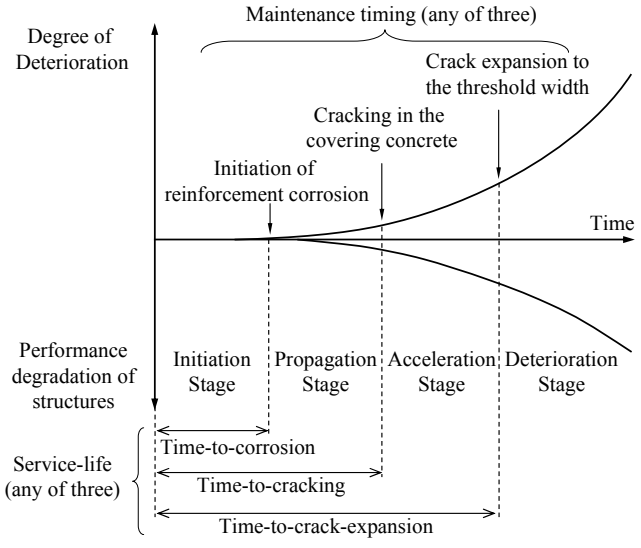

Figure 1 Deterioration process of RC structures

This study defines the elapsed time before a RC structure deteriorates to its maintenance criterion as the "service-life" of the structure and regards it as the timing of maintenance expenditures in LCCA. This study assumes that maintenance actions are carried out at any of *time-to-corrosion*, *time-to-cracking*, or *time-to-crack-expansion*, based on adopted maintenance policies.

2.2 Chloride-induced Deterioration Model

Figure 2 illustrates the chloride-induced deterioration model used in this study. This deterioration model formulates 1) chloride content at the surface of embedded reinforcement $C(x_c, t)$, 2) corrosion depth of reinforcement $\Delta D(t)$, and 3) crack width $W(t)$, as a function of time t.

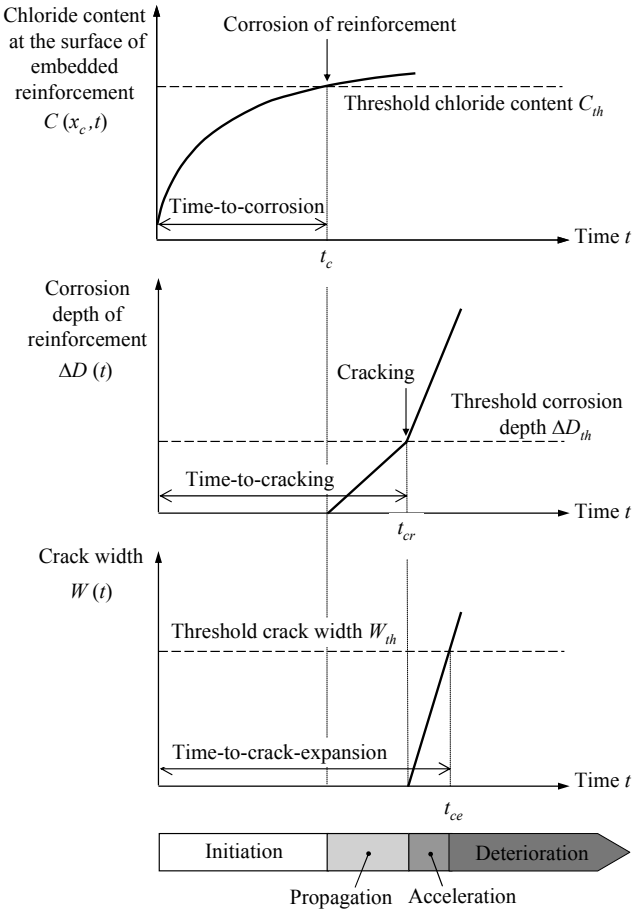

Figure 2 Chloride-induced deterioration model

In this model, the chloride content profile for a given year is calculated first. When the chloride content at the surface of embedded reinforcement $C(x_c, t)$ reaches the threshold level C_{th}, the reinforcement starts corroding. Then, the corrosion depth $\Delta D(t)$ is calculated; when it reaches the threshold level ΔD_{th}, cracking is induced in the covering concrete. Finally, the crack width $W(t)$ is computed until it reaches the threshold level W_{th}. Table 1 summarizes the predictive models and threshold values adopted in this study.

Table 1 Predictive models and threshold values

Parameters	Model/Value used
$C(x_c, t)$	Fick's Second Law of Diffusion
C_{th}	1.2-2.4kg/m^3 (JSCE)
$\Delta D(t)$	Bilinear model
ΔD_{th}	Bazant's model
$W(t)$	Linear model (Thoft-Christensen's model)
W_{th}	0.4-0.6mm (JCI)

2.2.1 Time-to-Corrosion

Chloride profile in concrete is modeled by means of *Fick's Second Law of Diffusion*, as follows:

$$C(x,t) = (C_s - C_i)\left[1.0 - erf\left(\frac{0.1x}{2\sqrt{D^* \cdot t}}\right)\right] + C_i \quad \text{(Eq.1)}$$

where

$C(x,t)$: Chloride content at depth (x) and time (t) (kg/m^3)

x : Depth from the concrete surface (mm)

t : Elapsed time (years)

C_s : Chloride content on the concrete surface (kg/m^3)

C_i : Content of initially-included chloride ions (kg/m^3)

D^* : Apparent diffusion coefficient of chloride ions (cm^2/year)

erf : Error function.

When the chloride content at the surface of the embedded reinforcement reaches the threshold value C_{th}, the corrosion of the reinforcement starts. Hence, the time-to-corrosion t_c can be estimated, as follows:

$$t_c = \frac{(0.1x_c)^2}{4\,D^*}\left[erf^{-1}\left(1 - \frac{C_{th} - C_i}{C_s - C_i}\right)\right]^{-2} \quad \text{(Eq.2)}$$

where

t_c: Time-to-corrosion (years)

x_c: Thickness of concrete cover (mm)

C_{th} : Threshold chloride content for the initiation of reinforcement corrosion (kg/m^3).

In Eq.2, the chloride content on the concrete surface C_s is determined by the distance from the coast (JSCE 2001). Furthermore, the apparent diffusion coefficient of chloride ions D^* is calculated as a function of the water-cement ratio of concrete, as follows (JSCE 2001):

$$\log D^* = -3.9\left(\frac{w_w}{w_c}\right)^2 + 7.2\left(\frac{w_w}{w_c}\right) - 2.5 \quad \text{(Eq.3)}$$

where

w_w: Water weight per unit volume (kg/m^3)

w_c: Cement weight per unit volume (kg/m^3).

2.2.2 Corrosion of Reinforcement

When the chloride content at the surface of the embedded reinforcement reaches the threshold value, the corrosion of the reinforcement starts. In this model, the corrosion depth of reinforcement $\Delta D(t)$ is used as an index that indicates the corrosion amount, and it increases linearly as time passes. Some previous studies claim that the corrosion rate leaps after crack generation (e.g., Morinaga 1996). In this study, therefore, the evolution of reinforcement corrosion is modeled with two lines; their slopes respectively represent the corrosion rate of reinforcement before and after cracking (α_1, α_2), as follows:

$$\Delta D(t) = \begin{cases} 0, & t \le t_c \\ \alpha_1 (t - t_c), & t_c < t \le t_{cr} \\ \alpha_2 (t - t_{cr}) + C, & t > t_{cr} \end{cases} \quad \text{(Eq.4)}$$

where

$\Delta D(t)$: Corrosion depth of reinforcement at time (t) (mm)

t_{cr}: Time-to-cracking (years)

α_1: Corrosion rate of reinforcement in uncracked concrete (mm/year)

α_2: Corrosion rate of reinforcement in cracked concrete (mm/year)

C: Constant $(= \alpha_1 (t_{cr} - t_c) = \Delta D_{th})$ (mm).

In Eq.4, the corrosion rates of reinforcement α_1 and α_2 are estimated by means of *Faraday's Law*, assuming that the current density in the reinforcing steel is constant and that the corrosion product is only iron(II) hydroxide $Fe(OH)_2$ for the sake of simplicity. In addition, Nakagawa et al. (2000) demonstrated that the corrosion rate of reinforcing steel in cracked concrete is 3.1 times faster than that in uncracked concrete. Given these points, α_1 and α_2 are respectively expressed by the following:

$$\alpha_1 = 1.16 \times 10^6 \cdot i_c \quad \text{(Eq.5)}$$

$$\alpha_2 = 3.60 \times 10^6 \cdot i_c \quad \text{(Eq.6)}$$

where

i_c: Current density in the reinforcing steel (before cracking) (A/mm^2).

2.2.3 Time-to-Cracking

When the corrosion depth of reinforcement reaches the threshold level, cracking appears in the covering concrete. In this study, the threshold corrosion depth is estimated by Bazant's model (1979) based on the *Thick-Wall Cylinder Theory*. In his model, the tensile stress induced into the cement paste is calculated by considering the volume change of the reinforcement before and after the corrosion.

Bazant's model identifies two crack modes: inclined cracking, in which planar cracks of a 45 degree inclination emanate from the surface of the reinforcement, and cover peeling, in which a crack runs parallel to the surface from one reinforcing bar to another. In this model, when the diameter of reinforcement increases by Δd_{th}, cracks are induced into the covering concrete. This threshold increase in the diameter of reinforcement Δd_{th} is expressed as:

$$\Delta d_{th} = \begin{cases} 2 f_t' \frac{x_c}{D_0} \delta_{pp}, & x_c < \frac{s - D_0}{2} \\ f_t' \left(\frac{s}{D_0} - 1 \right) \delta_{pp}, & x_c \ge \frac{s - D_0}{2} \end{cases} \quad \text{(Eq.7)}$$

where

Δd_{th}: Threshold increase in the diameter of reinforcement (including the thickness of produced rust) for cracking (mm)

s: Spacing of reinforcing steel (mm)

D_0: Original diameter of reinforcing steel (mm)

f_t': Tensile strength of concrete (N/mm^2) (=$0.23 f_c'^{2/3}$ (JSCE 2002))

f_c': Compressive strength of concrete (N/mm^2)

δ_{pp} : Bar hole flexibility (mm^3/N) $(= (1 + \nu) D_0 / E_{eff})$

ν: Poisson ratio of concrete

E_{eff}: Effective elastic modulus of concrete (N/mm^2) (=$E_c/(1 + \phi_{cr})$)

E_c: Elastic modulus of concrete (N/mm^2)

ϕ_{cr}: Creep coefficient of concrete.

This threshold value Δd_{th} represents the increase in the diameter of reinforcing steel *including produced rust*. Therefore, it can be converted into the corrosion depth of reinforcing steel ΔD_{th} by using the molar volume of steel V_{steel} and rust V_{steel}, as follows:

$$\Delta D_{th} = \left(\frac{V_s}{V_r - V_s} \right) \Delta d_{th} \quad \text{(Eq.8)}$$

where

ΔD_{th}: Threshold corrosion depth of reinforcement for cracking (mm)

V_s: Molar volume of steel (mm^3/mol) (= 7.097×10^3)

V_r: Molar volume of rust (mm^3/mol) (= 26.426×10^3).

As the discussion above shows, the time-to-cracking t_{cr} is estimated by substituting Eq.5 and Eq.8 into Eq.4, as follows:

$$t_{cr} = t_c + \frac{3.17\times10^{-7}\cdot\Delta d_{th}}{i_c} \quad \text{(Eq.9)}$$

2.2.4 Crack Expansion

After cracking appears in the covering concrete, the crack expands as the corrosion of reinforcement progresses. According to Thoft-Christensen (2003), the crack width increases linearly as the corrosion depth of reinforcement $\Delta D(t)$ increases. Therefore, crack width $W(t)$ is modeled as follows:

$$W(t) = \begin{cases} 0, & t \le t_{cr} \\ \gamma\cdot(\Delta D(t) - \Delta D_{th}), & t > t_{cr} \end{cases} \quad \text{(Eq.10)}$$

where

$W(t)$: Crack width at time (t) (mm)

γ: Crack evolution parameter

where

$$\gamma = \frac{(\beta-1)\pi D_0}{x_c}\cdot\frac{1}{\frac{D_0/2}{D_0/2+x_c}+1} \quad \text{(Eq.11)}$$

where

β: The ratio of the density of steel to that of rust product (=2.31).

Eq.10 is transformed by substituting Eq.4 and Eq.6, as:

$$W(t) = \begin{cases} 0, & t \le t_{cr} \\ 3.60\times10^6\cdot\gamma\cdot i_c(t-t_{cr}), & t > t_{cr} \end{cases} \quad \text{(Eq.12)}$$

2.2.5 Time-to-Crack-Expansion

In current practice, crack width is often used as a maintenance criterion of RC structures. For example, the Japan Concrete Institute (JCI) (2003) provides criteria for crack widths that do and do not require maintenance, depending on the environmental conditions. In this model, the time-to-crack-expansion to the threshold width t_{ce} is calculated by substituting $W(t) = W_{th}$ into Eq.12, as follows:

$$t_{ce} = t_{cr} + \frac{2.78\times10^{-7}\cdot W_{th}}{\gamma\cdot i_c} \quad \text{(Eq.13)}$$

where

t_{ce}: Time-to-crack-expansion (years)

W_{th}: Threshold crack width (mm).

3. PROBABILISTIC LCCA

3.1 Life-Cycle Cost

This study uses the *Net Present Value* in estimating the LCC of structures, as follows:

$$LCC = C_{t=0} + \sum_{t_i=1}^{N}\frac{C_{t=t_i}}{(1+i)^{t_i}} \quad \text{(Eq.14)}$$

where

LCC: Life-Cycle Cost (Net present value)

$C_{t=t_i}$: Total costs spent in year (t_i)

t_i: Timing of costs (year)

i: Discount rate (annual)

N: Analysis period (years) (=100).

Regarding the kinds of cost, construction, inspection, maintenance, and operation costs are considered in Eq.14. Furthermore, this study assumes that RC structures are used throughout the analysis period (=100 years) by repeating the same maintenance actions without being demolished. Therefore, the timing of maintenance costs is determined based on either time-to-corrosion t_c, time-to-cracking t_{cr}, or time-to-crack-expansion t_{ce}, which are respectively estimated by Eq.2, Eq.9, or Eq.13.

3.2 Framework of Probabilistic LCCA

So far, the concrete deterioration model and the LCC estimation have been formulated. This study adopts the Monte-Carlo Simulation method to assess the uncertainties of input parameters probabilistically. Figure 3 represents the overall LCCA framework, which consists of two steps of Monte-Carlo simulations: 1) the service-life estimation and 2) the LCC estimation.

In the first simulation, a set of values of uncertain variables is randomly sampled based on the probability distributions prescribed in advance. These values are entered into the concrete deterioration model. Through a large number of deterministic trials, three different service-lives (time-to-corrosion t_c , time-to-cracking t_{cr} , time-to-crack-expansion t_{ce}) of an intended structure are obtained as a form of probability distributions (see Figure 4).

The obtained probability distributions are then input in the second simulation as the timing of maintenance actions as well as other input variables. Again, through a large number of deterministic trials, the probability distribution of LCC is calculated.

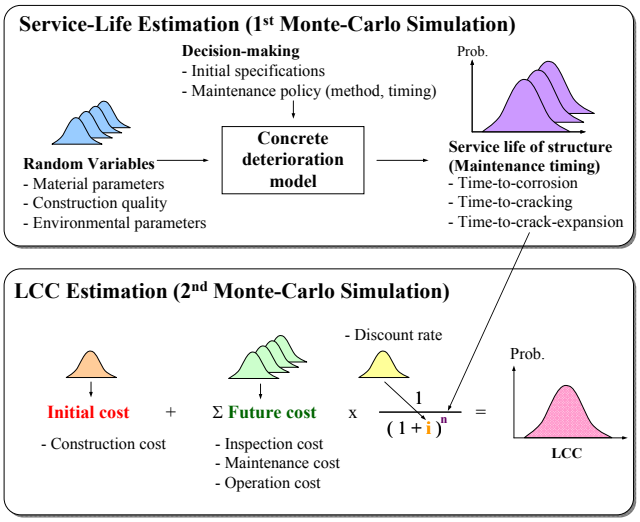

Figure 3 Probabilistic LCCA framework

4. CASE STUDY

This Section discusses a case study to which the developed probabilistic LCCA is applied. This case study also conducts a deterministic LCCA and discusses how the decision-making may differ between deterministic and probabilistic approach.

4.1 Structure and Life-Cycle Scenarios

Figure 5 illustrates a RC viaduct used in the case study, and Table 2 presents the general information about the viaduct.

Table 3 summarizes the eight potential life-cycle scenarios of the structure; each scenario has distinct initial specifications, maintenance

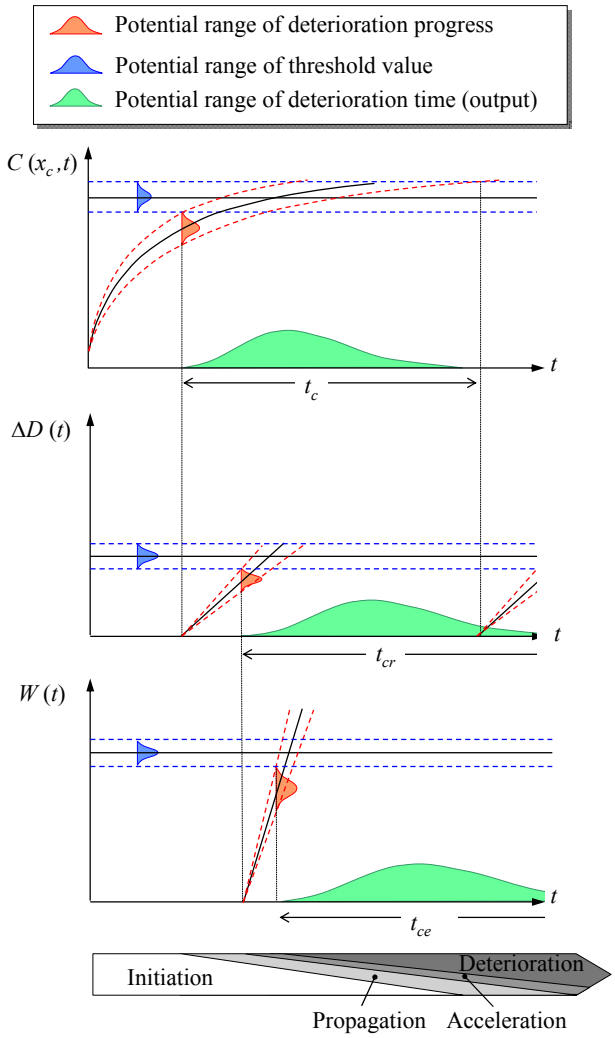

Figure 4 Application of the Monte-Carlo Simulation method to the deterioration model

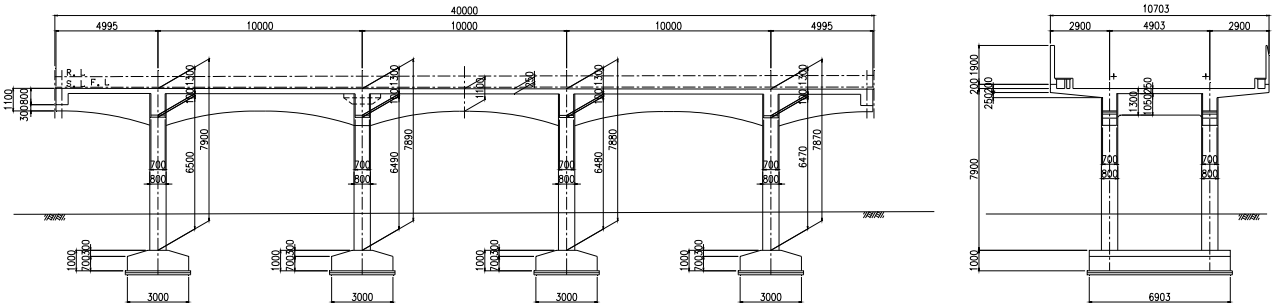

Figure 5 Target RC structure

Table 2 Information of the target structure

Length	40.0 m
Form area (superstructure)	826.9 m^2
Concrete volume (superstructure)	238.6 m^3
Weight of reinforcement (superstructure)	71.3 t
Design concrete strength (superstructure)	27 N/mm^2
Distance from coast	0.5 km

Table 3 Potential life-cycle scenarios

Case No.	Initial specification	Maintenance	
		Method	Timing
1	Normal	Desalination	t_c
2	Normal	Cathodic protection	t_{cr}
3	Normal	Patching	t_{ce}
4	Normal	Patching and Surface-coating	t_{ce}
5	Surface-coating	Surface-coating	t_{ce}
6	Epoxy-coated reinforcement (ECR)	Patching	t_{ce}
7	Fiber reinforced concrete (FRC)	Patching	t_{ce}
8	Cathodic protection	Cathodic protection	--

Table 4 Modeling of construction and maintenance technologies

Method	Way of modeling
Desalination	Chloride content in the covering concrete is restored to its initial state, also halting the corrosion of reinforcement.
Cathodic protection	The corrosion of embedded reinforcement is halted.
Patching	Chloride content in the covering concrete is restored to its initial state.
Surface-coating	The shielding effect of surface-coating membrane is converted to the equivalent concrete thickness with the thickness of membrane t_s and the apparent diffusion coefficient in the membrane D_s^* (JSCE 2003)
ECR	The shielding effect of epoxy-coating is converted to the equivalent concrete thickness with the thickness of epoxy-coating t_{ep} and the apparent diffusion coefficient in the epoxy-coating D_{ep}^* (JSCE 2005).
FRC	Crack evolution parameter γ is decreased to γ' (crack evolution parameter of FRC).

methods, and maintenance timing. This study assumes that the same maintenance methods are repeatedly applied to the structure under the same maintenance criteria in each scenario.

Among the maintenance methods in Table 3, some can be used as initial specifications of newly-built RC structures. For example, surface-coating method, epoxy-coated reinforcement (ECR), and fiber reinforced concrete (FRC) can be used in the construction to add extra durability in advance, and the cathodic protection system can be installed on RC structures to prevent the corrosion of reinforcement completely. These construction and maintenance methods are modeled by modifying the

baseline deterioration model described in Section 2 (see Table 4). On the whole, Cases 1-4 can be regarded as the scenarios taking corrective maintenance policies, and Cases 5-8 can be regarded as the ones taking more preventive policies.

4.2 Service-Life Estimation (1st Simulation)

Table 5 summarizes the parameters that prescribe the probability distributions of input variables used for service-life estimation. These parameters are determined primarily based on previous studies or standard specifications. This case study assumes that all input variables are independently random. Table 5 also includes the mean values input in the deterministic LCCA for the purpose of comparison in the following Sections.

Table 5 Input parameters for service-life estimation

	Probabilistic LCCA		Deterministic LCCA
	Type*	Parameters	
x_c	N	μ = 35.0, σ = 4.0	35.0
C_s	U	min = 1.8, max = 2.2	2.0
C_i	U	min = 0, max = 0.30	0.15
C_{th}	U	μ = 1.8, σ = 0.2	1.8
w_w	N	μ = 168, σ = 3.33	168
w_c	N	μ = 336, σ = 1.12	336
i_c	L	μ = 1.0×10^{-9}, σ = 5.0×10^{-10}	1.0×10^{-9}
f_c'	N	μ = 32.4, σ = 1.5	32.4
E_c	(N)	10,870 ln f_c' −9,170	28,638
D_0	C	19	19
s	N	μ = 250, σ = 12.5	250
ν	C	0.2	0.2
ϕ_{cr}	C	2.0	2.0
W_{th}	U	min = 0.3, max = 0.5	0.4
t_s	C	0.5	0.5
D_s^*	N	μ = 1×10^{-3}, σ = 5×10^{-5}	1×10^{-3},
t_{ep}	N	μ = 0.2, σ = 0.01	0.2
D_{ep}^*	N	μ = 2×10^{-6}, σ = 1×10^{-7}	2×10^{-6}
γ'	C	$\gamma\times$ 0.4	$\gamma\times$ 0.4

* N: Normal distribution U: Uniform distribution
L: Lognormal distribution C: Constant value

Figure 6 represents the result of the first Monte-Carlo simulation. As these graphs show, the potential ranges of the structure's service-life are considerably different depending on the initial specifications: accordingly, the probabilities that the viaduct requires maintenance actions within 100 years differ between 0% to 30.7% depending on the scenario. These probability distributions are used in the second simulations as a part of input parameters.

(1) Cases 1-4 (Normal specification)

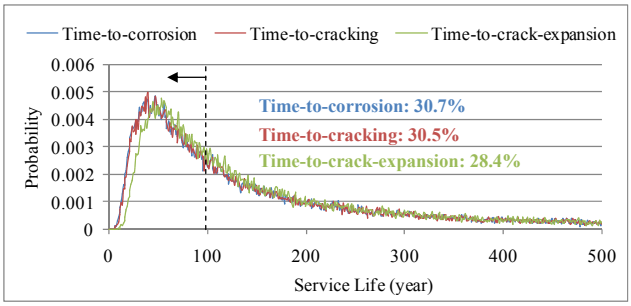

(2) Case 5 (Surface-coating)

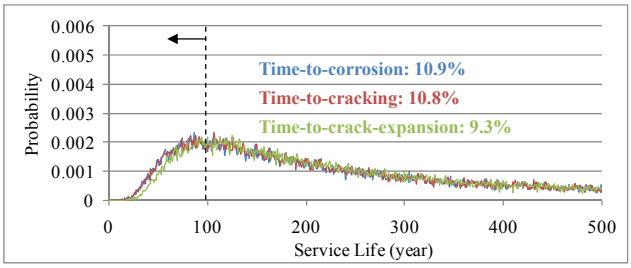

(3) Case 6 (ECR)

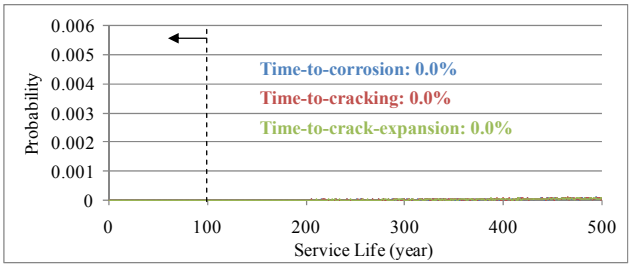

(4) Case 7 (FRC)

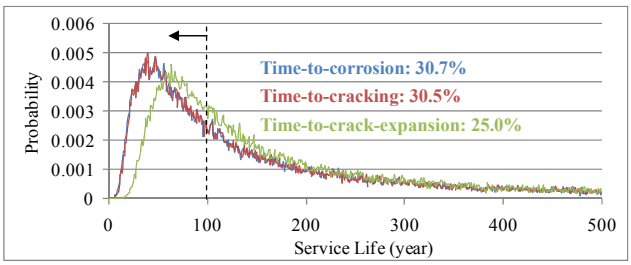

Figure 6 Simulated probability distributions of service-life in each scenario

Meanwhile, Table 6 summarizes the service-life obtained from the deterministic calculation. This Table indicates that the target viaduct does not require any maintenance actions within 100 years regardless of the adopted scenario.

Table 6 Estimated service-life by the deterministic calculation

Case No.	Time-to-corrosion	Time-to-cracking	Time-to-crack-expansion
1-4	248.7 years	249.3 years	255.3 years
5	575.8 years	576.4 years	582.5 years
6	+ 7,000 years	+ 7,000 years	+ 7,000 years
7	248.7 years	249.3 years	264.4 years

4.3 LCC Estimation (2nd Simulation)

Table 7 summarizes the parameters that prescribe the probability distributions of input variables for LCC estimation. Table 7 also includes the mean values used in the deterministic LCCA.

Figure 7 presents the probability distributions of LCC obtained through the second Monte-Carlo simulation. This Figure compares the potential ranges of LCC over the analysis period among the eight life-cycle scenarios. Although all of these probability distributions show bell-shapes, their geometric characteristics (i.e., mean, variation, skewness) are different, to a greater or lesser extent, depending on the particular scenario.

Table 7 Input parameters for LCC estimation

Type of costs	Variable	Unit	Probabilistic LCCA		Deterministic LCCA	Note
			Type*1	Parameters		
Construction	Normal	¥K/m	N	μ = 1,100, σ = 11.0	1,100	
	Surface-coating	¥K/m^2	N	μ = 12.5, σ = 0.125	12.5	(*2)
	Cathodic protection	¥K/m^2	N	μ = 55, σ = 0.55	55	(*3)
	ECR	¥K/t	N	μ = 72, σ = 0.72	72	
	FRC	¥K/m^3	N	μ = 1.0, σ = 0.01	1.0	0.5 vol%
	Indirect cost	% of direct cost	C	25%	25%	
Maintenance & Inspection	Surface-coating	¥K/m^2	N	μ = 12.5, σ = 0.25	12.5	(*2)
	Cathodic protection	¥K/m^2	N	μ = 55, σ = 1.1	55	(*3)
	Desalination	¥K/m^2	N	μ = 70, σ = 1.4	70	
	Patching	¥K/m^2	N	μ = 125, σ = 2.5	125	(*4)
	FRC (for Patching)	¥K/m^2	N	μ = 0.1, σ = 0.02	0.1	0.5vol% (*4)
	Scaffolding	¥K/m	N	μ =30, σ = 0.6	30	
	Routine inspection	¥K/time	N	μ = 30, σ = 0.3	30	Every 2 years
	Detailed inspection	¥K/time	N	μ = 100, σ = 1.0	100	Every 5 years
	Indirect cost	% of direct cost	C	40%	40%	
Operation	Cathodic protection	¥K/m^{2}year	N	μ = 1.0, σ = 0.02	1.0	Power supply
Others	Analysis period N	years	C	100	100	
	Discount rate i	%	T	min = 3.0, max = 5.0 mean = 4.0	4.0	

*1 N: Normal distributions, T: Triangle distributions, C: Constant value

*2 Requires the replacement of surface-coating membrane at least once in 50 years

*3 Requires the replacement of entire system every 40 years

*4 Patching area is assumed as; 25% of total area (1st patching), 50% (2nd patching), 100% (3rd patching and later).

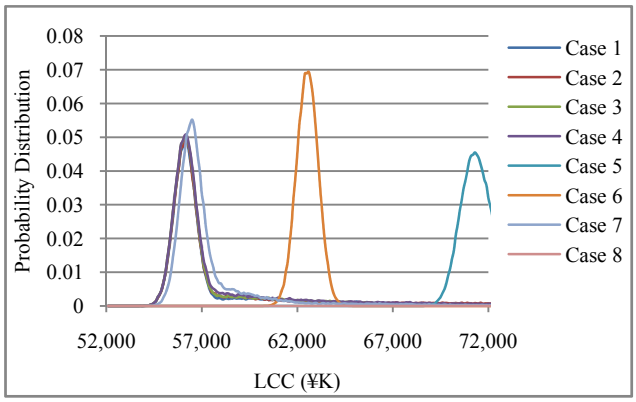

Figure 7 Simulated probability distributions of LCC (NPV basis) in each scenario

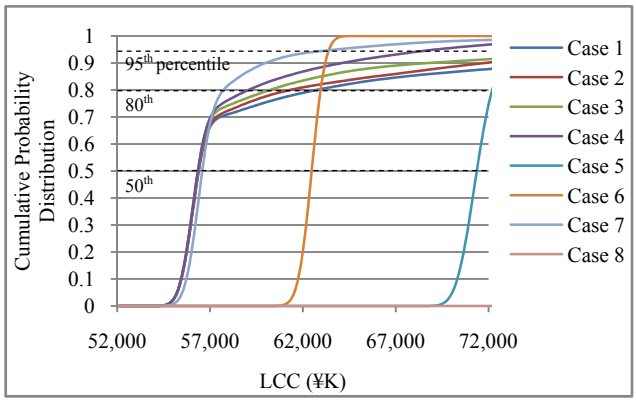

Figure 8 Simulated cumulative probability distributions of LCC (NPV basis) in each scenario

4.4 Selection of Life-Cycle Scenario

Since the probabilistic LCCA provides us with the potential ranges of LCC as an output, each alternative cannot be evaluated by superficially comparing the shape of the probability distributions. Instead, we need to scrutinize the potential risk, which is the increase in LCC beyond the permissible limit.

Figure 8 represents the simulated cumulative probability distributions of LCC under the eight life-cycle scenarios. Each line indicates the probability at which the LCC over the analysis period remains within a specific value. This criterial value differs depending on decision-makers' risk attitude (or budgetary constraints).

Table 8 summarizes the LCC at the 50th, 80th, and 95th percentiles in each scenario. As we can see in this Table, the life-cycle scenario with the lowest LCC differs depending on the decision-makers' criteria. For example, when the 50th percentile is used to evaluate these scenarios, Case 4, which adopts a corrective maintenance policy, has the lowest LCC. When the 80th percentile is adopted as a decision criterion, Case 7, which uses the FRC as initial specifications, is selected as the lowest LCC scenario. When the decision is made based on the 95th percentile, Case 6, which adopts the ECR, is selected.

Table 8 Estimated LCC (NPV basis) in the probabilistic and deterministic LCCA (unit: ¥K)

Case No.	Probabilistic LCCA			Deterministic LCCA
	50th percentile	80th percentile	95th percentile	
1	56,396	62,735	93,350	**56,052**
2	56,383	61,323	80,873	**56,052**
3	56,355	60,226	81,844	**56,052**
4	**56,351**	59,075	69,143	**56,052**
5	71,371	72,200	73,991	71,245
6	62,481	62,959	**63,419**	62,469
7	56,587	**57,734**	63,811	56,350
8	150,440	155,457	160,505	150,439

* Underlined scenarios have the lowest LCC under each decision-making criterion

Thus, this case study has shown quantitatively that if a decision-maker is relatively "risk-neutral" and his/her decision is made based on the most probable LCC, he/she should construct the viaduct with standard specifications and repeat corrective maintenance actions, as seen in Case 4. On the other hand, if the decision-maker has more "risk-averse" standpoint and wishes to alleviate the risks of LCC increase, he/she should add extra durability to the viaduct through the construction and decrease the risks of rapid deterioration, as seen in Cases 6 and 7. In addition, the selection of life-cycle scenario differs depending on the degree of decision-maker's

tolerance against the risks.

Under the given conditions, some of the positive protective systems, such as FRC and ECR, could effectively alleviate the risks of potential increase in LCC. It should be noted, however, that other positive protection systems such as surface-coating and cathodic protection are not cost-effective in the given conditions due to their upfront expenditure.

4.5 Effectiveness of Probabilistic LCCA

As well as three different percentiles calculated from the probabilistic LCCA, Table 8 includes the result of the deterministic LCCA. When we compare the result of deterministic LCCA with a specific percentile in the probabilistic LCCA, we can recognize that the deterministic approach gives us a similar result with the 50th percentile (i.e., median) in the probabilistic approach.

As we discussed with respect to Table 6, the deterministic approach predicts that the viaduct does not require any maintenance actions within 100 years regardless of the initial specifications; therefore, standard specifications are chosen as the most cost-effective initial specifications of the viaduct. However, the deterministic LCCA does not take the downward risks into account, and therefore, it is not always an effective decision-making method especially for risk-averse decision-makers. In such cases, instead, the probabilistic LCCA exhibits its effectiveness because it can help in avoiding the potential risks of cost overrun by assessing the potential ranges of LCC in each life-cycle scenario.

5. CONCLUSION

This study has developed a probabilistic framework to estimate the LCC of RC structures under various construction and maintenance scenarios. Then, the developed framework is applied to a RC viaduct under chloride-dominant environment as a case study. The case study has shown that some preventive maintenance policies can effectively mitigate the risk of LCC increase.

This study indicates that the developed probabilistic LCCA framework can be used as an effective method for identifying the most cost-effective life-cycle scenarios, considering the downward risks of an increase in LCC and reflecting the risk attitude of the decision-maker. With this framework, we can comprehensively design the life-cycle scenario of concrete infrastructures in terms of risk control from the preliminary design stages in construction projects.

REFERENCES

Bazant, Z. P. (1979). “Physical model for steel corrosion in concrete sea structures-application.” Journal of the Structural Division, Vol.105, No.6, 1155-1166.

Japan Concrete Institute (2003). Practical Guideline for Investigation, Repair and Strengthening of Cracked Concrete Structures -2003-, Tokyo, Japan.

Japan Society of Civil Engineers (2001). Standard Specification for Concrete Structures-2001 "Maintenance," Tokyo, Japan.

Japan Society of Civil Engineers (2002). Standard Specification for Concrete Structures-2002 "Materials and Construction," Tokyo, Japan.

Japan Society of Civil Engineers (2003). Recommendation for Design and Construction of Concrete Structures Using Epoxy-Coated Reinforcing Steel Bars, Revised Edition, Concrete Library 112, Tokyo, Japan.

Japan Society of Civil Engineers (2005). Recommendation for Concrete Repair and Surface Protection of Concrete Structures, Concrete Library 119, Tokyo, Japan.

Morinaga, S. (1996). “Remaining life of reinforced concrete structures after corrosion cracking.” Durability of Building Materials and Components, C. Sjostrom, eds., E&FN Spon, London, UK, 127-137.

Nakagawa, T., Tsutsumi, T., & Matsushima, M. (2000). “Engai-rekka o ukeru RC kouzoubutsu no rekka-yosoku.” Journal of Concrete Research and Technology, Vol.22, No.1, Japan Concrete Institute, 415-420 (in Japanese).

Thoft-Christensen, P. (2003).”Corrosion and cracking of reinforced concrete.” Life-Cycle Performance of Deteriorating Structures: Assessment, Design, and Management, D. M. Frangopol, E. Bruhwiler, M. H. Faber, & B. Adey, eds., American Society of Civil Engineers, Reston, VA, 26-36.